Metabolism Clinical and Experimental 96 (2019) 12–21

Contents lists available at ScienceDirect

Metabolism Clinical and Experimental

journal homepage: www.metabolismjournal.com

Fatty acid binding protein 4 (FABP4) as a potential biomarker reflecting myocardial lipid storage in type 2 diabetes

Ricardo Rodríguez-Calvo [a,b,*], Josefa Girona [a,b], Marina Rodríguez [a,b], Sara Samino [b,c], Emma Barroso [b,d,e], David de Gonzalo-Calvo [f,g], Sandra Guaita-Esteruelas [a,b], Mercedes Heras [a,b], Rutger W. van der Meer [h], Hildo J. Lamb [h], Oscar Yanes [b,c], Xavier Correig [b,c], Vicenta Llorente-Cortés [f,g,i], Manuel Vázquez-Carrera [b,d,e], Lluis Masana [a,b,*]

[a] Vascular Medicine and Metabolism Unit, Research Unit on Lipids and Atherosclerosis, "Sant Joan" University Hospital, Universitat Rovira i Virgili, Institut de Investigació Sanitaria Pere Virgili (IISPV), Reus, Spain
[b] Spanish Biomedical Research Centre in Diabetes and Associated Metabolic Disorders (CIBERDEM), Institute of Health Carlos III, Madrid, Spain
[c] Metabolomics Platform, Department of Electronic Engineering (DEEEA), Universitat Rovira i Virgili, Tarragona, Spain
[d] Pharmacology Unit, Department of Pharmacology, Toxicology and Therapeutic Chemistry, Faculty of Pharmacy and Food Sciences, Institut de Biomedicina de la Universidad de Barcelona (IBUB), University of Barcelona, Barcelona, Spain
[e] Institut de Recerca Sant Joan de Déu (IR-SJD), Barcelona, Spain
[f] Lipids and Cardiovascular Pathology Group, Biomedical Research Institute Sant Pau (IIB Sant Pau), Barcelona, Spain
[g] Network Spanish Biomedical Research Centre for Biomedical Research in Cardiovascular Diseases (CIBERCV), Institute of Health Carlos III, Madrid, Spain
[h] Department of Radiology, Leiden University Medical Centre, Leiden, the Netherlands
[i] Biomedical Research Institute of Barcelona, CSIC, Barcelona, Spain

ARTICLE INFO

Article history:
Received 15 January 2019
Accepted 8 April 2019

Keywords:
Myocardial neutral lipid content
FABP4
Cardiac lipotoxicity
Insulin resistance
BMS309403

ABSTRACT

Objective: Fatty acid binding protein 4 (FABP4) is an intracellular lipid chaperone involved in the crosstalk between adipose and peripheral tissues, and it contributes to widespread insulin resistance in cells, including cardiac cells. However, the role of this adipokine in regulating cardiac metabolism and myocardial neutral lipid content in patients with type 2 diabetes has not been elucidated.

Methods: The impact of circulating FABP4 on the cardiac neutral lipid content was measured by proton magnetic resonance spectroscopy (^{1}H-MRS) in patients with type 2 diabetes. Additionally, circulating FABP4 and the cardiac triglyceride content were analysed in high-fat diet (HFD)-fed mice, and the impact of the exogenous FABP4 was explored in HL-1 cardiac cells.

Results: Serum FABP4 levels were higher in type 2 diabetic patients compared to healthy individuals. Circulating FABP4 levels were associated with myocardial neutral lipid content in type 2 diabetic patients. In HFD-fed mice, both serum FABP4 and myocardial triglyceride content were increased. In FABP4-challenged HL-1 cells, extracellular FABP4 increased intracellular lipid accumulation, which led to impairment of the insulin-signalling pathway and reduced insulin-stimulated glucose uptake. However, these effects were partially reversed by FABP4 inhibition with BMS309403, which attenuated the intracellular lipid content and improved insulin signalling and insulin-stimulated glucose uptake.

Conclusions: Taken together, our results identify FABP4 as a molecule involved in diabetic/lipid-induced cardiomyopathy and indicate that this molecule may be an emerging biomarker for diabetic cardiomyopathy-related disturbances, such as myocardial neutral lipid accumulation. Additionally, FABP4 inhibition may be a potential therapeutic target for metabolic-related cardiac dysfunctions.

1. Introduction

Obesity, particularly visceral fat accumulation, has been closely related to a wide range of metabolic disturbances, including insulin resistance/type 2 diabetes and cardiovascular diseases (CVD) [1]. The main cardiac disease associated with these pathologies is coronary artery disease, which usually leads to heart failure [2]. However, heart failure has been

* Corresponding authors at: Vascular Medicine and Metabolism Unit, Research Unit on Lipids and Atherosclerosis, "Sant Joan" University Hospital, Universitat Rovira i Virgili, Institut de Investigació Sanitaria Pere Virgili (IISPV), Reus, Spain.
E-mail addresses: ricardo.rodriguez@ciberdem.org (R. Rodríguez-Calvo), luis.masana@urv.cat (L. Masana).

https://doi.org/10.1016/j.metabol.2019.04.007
0026-0495/

associated with metabolic-related disturbances independently of vascular lesions [3]. Despite the risk of heart failure independent of the ischaemic pathology is not yet established, diabetic patients are at a two- to five-fold increased risk of heart failure [4]. Additionally, the incidence of heart failure attributed to obesity is estimated to increase by 5–7% per unit increase in body mass index (BMI) [5]. Ectopic fat accumulation in non-adipose tissues has been related to an altered cardiac structure, thus increasing the risk of cardiometabolic events [1]. At the cellular level, adipocytes act as endocrine organs, releasing fatty acids, proinflammatory mediators and other biological active molecules (adipokines) that target peripheral tissues to regulate cellular responses into the bloodstream. Thus, these molecules take part in a communication network between adipose tissue and peripheral organs, including the heart [6]. Among their other functions, both fatty acids and adipokines control energy metabolism in their target tissues and regulate substrate preferences for energy production. Specifically, several of these molecules directly influence the development of insulin resistance, thus increasing fatty acid utilization to the detriment of glucose uptake. In insulin-resistant cardiomyocytes, fatty acid uptake frequently exceeds mitochondrial β-oxidative capacity [7], thus promoting intramyocellular lipid accumulation and lipotoxicity, which further contributes to insulin resistance by directly impairing insulin-stimulated glucose uptake [8]. Augmented neutral lipid accumulation in the myocardium is commonly termed myocardial steatosis. Myocardial steatosis has been observed in patients with non-ischaemic cardiomyopathy in the terminal state [9], and it is independently associated with impaired contractile function and with the onset of myocardial dysfunction [10–13]. However, the clinical determination of the cardiac content of neutral lipids by proton magnetic resonance spectroscopy (^{1}H-MRS) is currently impractical for the screening of large populations. Thus, the identification of circulating molecules able to reflect the myocardial neutral lipid content would contribute to targeting of cardiac fat accumulation-related disturbances before they can become established.

Among the large number of adipokines produced by adipocytes, fatty acid binding protein 4 (FABP4) has been recently proposed as an emerging molecule involved in the development of metabolic and CVD (for review see [14]). FABP4 (A-FABP or aP2) is an intracellular lipid chaperone that is able to reversibly bind to hydrophobic ligands [15,16]. Thereby, FABP4 regulates lipid trafficking and cellular responses [17,18] and takes part in both lipid metabolism and insulin sensitivity regulation [19]. Additionally, it has been detected in the bloodstream and is able to induce responses in peripheral organs. Circulating FABP4 has been associated with metabolic syndrome and type 2 diabetes in several studies [20–22]. Furthermore, FABP4 has been directly related to cardiac alterations [14,23]. FABP4 levels are related to altered left ventricle structure and function [23–28], and serum FABP4 concentrations have been directly associated with heart failure [23,25,29–31]. FABP4 is induced in epicardial adipose tissue from metabolic syndrome subjects [32], which suggests a paracrine effect on cardiac cells. In animal models, FABP4 overexpression exacerbates cardiac hypertrophy induced by pressure overload [33], and FABP4 deficiency improves left ventricular function and reduces myocardial injury induced by ischaemia/reperfusion in both non-diabetic and streptozotocin-induced diabetic mice [34]. Moreover, FABP4 suppresses cardiomyocyte contraction [35], which shows a cause-effect relationship between FABP4 and cardiomyocyte physiology. However, the role of this molecule as a potential biomarker for myocardial neutral lipid content in type 2 diabetic patients has not been established, and the molecular mechanisms by which FABP4 regulates heart function are only beginning to emerge. It has been proposed that FABP4 may contribute to trans-endothelial fatty acid transport [36], thus regulating fatty acid delivery inside cardiomyocytes. Nevertheless, the role of FABP4 in regulating intramyocellular lipid content and insulin resistance in cardiomyocytes remains unknown.

In this work, we add a new piece to the puzzle and show that FABP4 induces intramyocellular lipid accumulation and contributes to insulin resistance in cardiac cells. Additionally, we show that circulating FABP4 is associated with myocardial neutral lipid content in well-controlled uncomplicated type 2 diabetes with verified absence of structural heart disease or inducible ischaemia [37]. Thereby, FABP4 may induce dysregulation of cardiac metabolism, which is a key mechanism in the development of adverse cardiac disturbances in diabetic subjects.

2. Material and Methods

2.1. Patients

Cardiac neutral lipid content was determined by ^{1}H-MRS in seventy-four men with uncomplicated type 2 diabetes and 12 age- and BMI-matched non-diabetic controls [13]. Patients were recruited from those participating in the PIRAMID (Pioglitazone Influence on tRiglyceride Accumulation in the Myocardium In Diabetes) study [37]. Data from these patients, including age, body mass index (BMI [weight (kg)/length (m^2)] and waist circumference were collected. The inclusion and exclusion criteria have been published elsewhere [37]. In brief, the inclusion criteria were age between 45 and 65 years, glycohaemoglobin levels from 6.5% to 8.5% at screening, BMI from 25 to 32 kg/m^2, and blood pressure below 150/85 mm Hg (both with or without the use of antihypertensive drugs). Subjects with any clinically significant disorder, particularly any history or complaint of cardiovascular or liver disease or diabetes-related complications, prior use of thiazolidinediones or insulin were excluded from the study. Absence of structural heart disease or inducible ischaemia was verified in these patients. Written informed consent was obtained from all participants. The study was approved by local ethics committees (Leiden University Medical Center and Vrije Universiteit Medical Center) and was performed in full compliance with the Declaration of Helsinki.

2.2. Biochemical and Imaging Studies in Patients and Controls

Blood samples were collected for substrate determination. Glucose, glycated haemoglobin (HbA1c), insulin, non-esterified fatty acids (NEFAs), total cholesterol, high-density lipoprotein (HDL)-cholesterol, low-density lipoprotein (LDL)-cholesterol, non-HDL-cholesterol, triglycerides, ultra-sensitive C-Reactive Protein (us-CRP), leucocyte count and N-terminal pro B-type natriuretic peptide (NT-proBNP) were previously determined [37,38]{van der Meer, 2009 #212}. Additionally, serum FABP4 levels were determined using a commercial enzyme-linked immunoabsorbent assay (Biovendor, Brno, Czech Republic).

Left ventricular (LV) mass, LV end-diastolic volume, LV end-systolic volume and stroke volume were calculated using magnetic resonance imaging (MRI). During MR examinations, both systolic and diastolic blood pressures and heart rate were monitored. LV ejection fraction and cardiac index (cardiac index = cardiac output/body surface area) were used as measures of systolic function. Determination of LV diastolic function parameters, including peak filling rates of the early filling phase (E) and atrial contraction (A) and their ratio (E/A) were calculated by measuring blood flow across the mitral valve by an electrocardiograph (ECG)-gated gradient echo sequence with velocity encoding. LV filling pressures (E/Ea) [39] and the peak (E-decpeak) and mean (E-decmean) deceleration gradients of E [40] were calculated. Both subcutaneous and visceral abdominal fat volumes were quantified by MRI as previously described [41]. All images were quantitatively analysed using the MASS and FLOW software (Medis, Leiden, the Netherlands).

Both Hepatic and Cardiac neutral lipid content was determined using ^{1}H-MRS as previously described [40,42]. Briefly, myocardial ^{1}H-MRS spectra were obtained from the interventricular septum, avoiding contamination from epicardial fat. Spectroscopic data acquisition was double-triggered with ECG triggering and respiratory navigator echoes to minimize motion artefacts. Water-suppressed spectra were acquired to measure myocardial triglyceride content using spectra without water

suppression as an internal standard [40]. Myocardial neutral lipid content was calculated as previously described [40,43]. Liver ^{1}H-MRS spectra was performed avoiding gross vascular structures and adipose tissue depots. All ^{1}H-MRS spectroscopic data were fitted by use of Java-based MR user interface software (jMRUI version 2.2) [43].

2.3. Animal Model Experiments

Six-week-old C57BL/6J male mice (Charles River Laboratories, Spain) were maintained on standard light–dark cycle (12 h light/dark cycle) and temperature (21 ± 1 °C) conditions with ad libitum access to food and water. The animals were randomly distributed in two experimental groups ($n = 10$ each) and fed a standard chow diet (STD: 10% kcal from fat; Panlab; Barcelona, Spain) or a high-fat diet (HFD: 60% kcal from fat; Panlab; Barcelona, Spain) for 12 weeks [44]. Before the end of the procedure, a glucose tolerance test (GTT) was performed on mice that were fasted for 4 h. Briefly, animals received 2 g/kg body weight of glucose by intraperitoneal injection, and blood was collected from their tail veins after 0, 15, 30, 60, 120 and 180 min. The area under the curve (AUC) was determined as a measure of glucose intolerance. After this period the mice were euthanized, and the heart was immediately frozen in liquid nitrogen and stored at −80 °C. A blood sample was collected, and plasma samples were analysed for glucose (Spinreact; Barcelona, Spain), insulin, resistin, leptin, adiponectin (Milliplex®, Millipore; Billerica, MA, USA), FABP4 (Biovendor; Brno, Czech Republic), NEFAs (Wako; Osaka, Japan) and triglycerides (Spinreact; Barcelona, Spain). To assess insulin sensitivity, the homeostatic model assessment (HOMA) index was calculated using the following equation: [fasting glucose (mmol/l) × fasting insulin (μU/ml)]/22.5 [45]. Myocardial triglyceride content was analysed by liquid chromatography/mass spectrometry (LC/MS). These experiments conformed to the Guide for the Care and Use of Laboratory Animals published by the U.S. National Institutes of Health (NIH publication no. 85-23, revised 1996). All procedures were approved by the University Rovira i Virgili Bioethics Committee, as stated in Law 5/21 July 1995 passed by the Generalitat de Catalunya (Autonomous Government of Catalonia).

2.4. Cell Culture Experiments

HL-1 atrial cardiomyocytes (from Dr. W. Claycomb laboratory, Louisiana State University, New Orleans, LA, USA) were cultured in Claycomb medium (supplemented with 10% fetal calf serum (FCS), 0.1 mmol/l noradrenaline [norepinephrine], 2 mmol/l L-glutamine, 100 U/ml penicillin and 100 μg/ml streptomycin) at 37 °C and 5% CO_2 as previously described [46,47]. Cells were seeded in multi-well plates and serum deprived in Dulbecco's Modified Eagle Medium (DMEM; supplemented with 2 mM L-glutamine, 100 μM non-essential amino acids (NEAA), 100 U/ml penicillin and 100 μg/ml streptomycin) for 24 h, and then stimulated with recombinant FABP4 (Biovendor Brno, Czech Republic) at 5 μg/ml for 8 or 24 h, in the presence or absence of BMS309403 (Tocris Bioscience, Bristol, UK) (25 μM). When indicated, the cells were acutely stimulated with insulin (Sigma-Aldrich, Madrid, Spain) (200 nmol/l, 10 min). After incubation, RNA, whole protein or membrane protein was extracted as described below.

2.5. Lipid Content Determination

Lipid content was measured in 5 mm cross-sections from frozen mouse hearts using Oil Red O stain following the protocol described by Mehlem et al. [48]. To visualize the lipid droplets in HL-1 cells, the lipophilic fluorescent dye Nile red (Sigma-Aldrich; Barcelona, Spain) was used [49]. Pictures were captured using a microscope (Olympus IX71, Spain). The lipid content from HL-1 cells was quantified with ImageJ software from four random fields.

2.6. Metabolomics

Lipids were extracted in methanol 0.1% formic acid. After sample fragmentation by vortexing, immersion in liquid N_2 and ultrasonication, 3 volumes of dichloromethane and 1 volume of water were added sequentially. Samples were incubated at 4 °C for 30 min and centrifuged (15,000 rpm, 15 min at 4 °C). The organic phase (lipidic) was collected for drying under a stream of nitrogen. Lipid pellets were resuspended in methanol:toluene (9:1) for LC/MS analysis.

Untargeted LC/MS analyses were performed using a UHPLC system (1200 series, Agilent Technologies) coupled to a 6550 ESI-QTOF MS (Agilent Technologies) operating in positive (ESI+) electrospray ionization mode. Lipids were separated by reverse phase chromatography with an Acquity UPLC C18-RP (ACQUITY UPLC BEH C18 1.7 μM, Waters). Mobile phase A was acetonitrile/water (60:40) (10 mM ammonium formate) and B was isopropanol/acetonitrile (90:10) (10 mM ammonium formate). Solvent modifiers were used to enhance ionization, as well as to improve the LC resolution in positive ionization modes. The separation was conducted under the following gradient: 0 in 15% of B; 0–2 min 30% of B; 2–2.5 min 48% of B; 2.5–11 min 82% of B; 11–11.5 min 99% of B; 11.5–12 99% of B; 12–12.1 min 15% of B; 12.1–15 min 15% of B. The ESI conditions were as follows: gas temperature, 150 °C; drying gas, 13 l min^{-1}; nebulizer, 35 psig; fragmentor, 150 V; and skimmer, 65 V. The instrument was set to work over the m/z range from 50 to 1200 with an acquisition rate of 3 spectra/s. For compound identification, MS/MS analyses were performed in targeted mode, and the instrument was set to acquire spectra over the m/z range from 700 to 900, with a default iso width (the width at half-maximum of the quadrupole mass bandpass used during MS/MS precursor isolation) of 4 m/z. The collision energy was fixed at 20 V.

LC/MS data were processed using XCMS [50] software (version 1.34.0) to detect and align mzRT features. XCMS analysis of these data provided a matrix containing the retention time, m/z value, and integrated peak area of each feature for each sample of cells and culture medium. We constrained the initial number of features by means of the following criteria: only features above an intensity threshold of 5000 for the analysis of the cell pellet were retained for further statistical analysis. Quality control samples (QCs) consisting of pooled cells samples from each condition were injected at the beginning and periodically through the worklist. The performance of the LC/MS platform for each mzRT feature detected in samples was assessed by calculating the relative standard deviation of these features on pooled samples (CVQC) [51].

2.7. RNA Preparation and Quantitative Real Time Reverse Transcription-Polymerase Chain Reaction (RT-PCR) Analysis

Levels of mRNA were assessed by real time RT-PCR as previously described [46]. Total RNA was isolated using the PureLink® RNA Mini Kit (Invitrogen, Life Technologies; Madrid, Spain) according to the manufacturer's recommendations. RNA integrity was determined by electrophoresis in agarose gel and was quantified by a NanoDrop 1000 Spectrophotometer (Thermo Scientific; Madrid, Spain). Total RNA (1 μg) was reverse-transcribed using the PrimeScript RT Reagent Kit (Takara Bio; France). Levels of mRNA were assessed by real-time PCR on an ABI PRISM 7900 sequence detector (Applied Biosystems; CA, USA). TaqMan gene expression assays-on-demand (IDT; Leuven, Belgium) were used for mouse *Cd36* (Mm.PT.58.7548967), mouse *Fabp4* (Mm.PT.58.43866459), mouse acyl-Coenzyme A (CoA) synthetase (*Acs*) (Mm.PT.58.29312796), mouse medium-chain acyl-CoA dehydrogenase (*Acadm*) (Mm.PT.58.9004416), mouse vey-long-chain acyl-CoA dehydrogenase (*Acadvl*) (Mm.PT.58.30103666), mouse acyl-CoA oxidase 1 (*Acox1*) (Mm.PT.58.5874703), mouse fatty acid synthase (*Fas*) (Mm.PT.58.14276063), mouse stearoyl-CoA desaturase 1 (*Scd1*) (Mm.PT.58.8351960), mouse glycerol-3-phosphate acyltransferase (*Gpat1*) (Mm.PT.58.12176691), mouse diacylglycerol O-acyltransferase 2

(*Dgat2*) (Mm.PT.58.28629966), mouse glucose transporter 4 (*Glut4*) (Mm.PT.58.9683859) and mouse pyruvate dehydrogenase kinase 4 (*Pdk4*) (Mm.PT.58.9453460). TATA-binding protein (*Tbp*) (Mm. PT.58.10867035) was used as the endogenous control [52,53].

2.8. Immunoblotting

HL-1 cells were challenged with 200 nmol/l insulin for 10 min. Whole cellular extracts were collected in RIPA buffer (0.1% SDS, 150 mM NaCl, 1% Nonidet P40, 50 mM Tris-HCl, 0.5% deoxycholate) containing phosphatase and protease inhibitors (Roche Diagnostics; Basel, Switzerland) [49]. To obtain membrane fraction proteins, cells were lysed in cold buffer (50 mM Tris–HCl, pH 7.4, 150 mM NaCl, 2 mM Ca2+, 1% Triton X-100, 1% NP40), and protease inhibitor cocktail (Roche, Indianapolis, IN, USA) for 15 min. Then, cell lysates were centrifuged at 16,000 ×*g* for 15 min, and the supernatants containing membrane proteins were collected [54]. Protein concentration was measured using a Bradford Assay Kit (Bio-Rad; USA), and equal amounts were resolved by sodium dodecyl sulphate-polyacrylamide gel electrophoresis (SDS-PAGE) and transferred to Immobilon polyvinylidene difluoride (PVDF) membranes using iBlot® Dry Blotting System (Life Technologies; Madrid, Spain). Western blot analyses were performed using antibodies against suppressor of cytokine signalling 3 (SOCS3), phospho-signal transducer and activator of transcription 3 (STAT3)^{Tyr705}, phospho-STAT3^{Ser727}, STAT3, phospho-AKT^{Ser473}, AKT, phospho-AS160^{Thr642} (AKT substrate of 160 kDa) and AS160, all of them from Cell Signalling (Beverly, MA, USA). FABP4, α-actin and GLUT4 antibodies were obtained from R&D Systems (Minneapolis, MN, USA), Santa Cruz Biotechnology (Santa Cruz, CA, USA) and Abcam (Cambridge, UK), respectively. Equal protein loading was verified using α-actin immunoblotting or Ponceau staining. Detection was performed using the appropriate horseradish peroxidase (HRP)-conjugated secondary antibody (Dako; Glostrup, Denmark). The bands were visualized using ECL reagents (Amersham Pharmacia; USA) with the Amersham Imager 600 and quantified with ImageQuant TL software, version 8.1 (GE Healthcare; Barcelona, Spain).

2.9. Glucose Uptake

Determination of glucose uptake was performed as previously described [55]. Briefly, glucose uptake was assayed using [^{3}H]2-deoxyglucose (2-DG). Cells were stimulated with recombinant FABP4 for 24 h and then challenged with 200 nM insulin for 30 min. After they were washed two times with wash buffer [20 mM HEPES (pH 7.4), 140 mM NaCl, 5 mM KCl, 2.5 mM $MgSO_4$, and 1 mM $CaCl_2$], cells were incubated in buffer transport solution (wash buffer containing 0.5 mCi [^{3}H]2-DG/ml and 10 μM 2-DG) for 20 min. Uptake was terminated by aspiration of the solution. Cells were then washed three times, lysed with 0.2 M NaOH, and incorporated glucose was measured by scintillation counting of ^{3}H in a β-counter. Data were normalized by the protein content.

2.10. Statistical Analysis

Data from experimental studies are expressed as the mean ± standard error mean (SEM) of at least 3 separate experiments. Significant differences were established by Student's *t*-test. Data were analysed by using the GraphPad Instat programme (GraphPad Prism 60.1 Software Inc.; La Jolla, CA, USA).

Data from clinical studies are expressed as scatter plots. The Kolmogorov-Smirnov test was used to assess the normality distribution of the variables. Continuous variables that were not normally distributed were compared between groups using the Mann-Whitney *U* test. Correlations were evaluated using Spearman's test. Data are presented using the Spearman's Rho coefficient. Statistical analyses were performed using SPSS software (IBM SPSS Statistics, version 22.0).

Differences were considered statistically significant at $P < 0.05$.

3. Results

3.1. Circulating FABP4 Protein Levels Are Associated With Myocardial Neutral Lipid Content in Patients With Uncomplicated Type 2 Diabetes

We first explored whether circulating FABP4 was associated with myocardial neutral lipid content in a population of well-characterized patients with controlled type 2 diabetes from the PIRAMID study [37,56]. Our data revealed elevated FABP4 protein levels in the serum from type 2 diabetes patients compared with healthy volunteers (non-T2D: 18.76 ± 1.42 ng/ml; T2D: 24.72 ± 1.08 ng/ml, $P < 0.05$). To analyse whether the serum FABP4 levels were related to characteristics of the type 2 diabetes population, we evaluated the association between this molecule and clinical, biochemical, metabolomics and haemodynamic parameters, as well as cardiac function and dimensions (Table 1). Serum FABP4 levels were positively correlated to waist circumference ($r = 0.359$, $P = 0.002$) and both visceral ($r = 0.383$, $P = 0.001$) and subcutaneous ($r = 0.404$, $P < 0.001$) fat volume, and they were inversely associated with high-density lipoprotein (HDL) cholesterol ($r = -0.235$, $P = 0.047$) in type 2 diabetes patients. Additionally, associations between FABP4 and HbA1c ($r = 0.201$, $P = 0.086$), fasting insulin ($r = 0.201$, $P = 0.087$), low-density lipoprotein (LDL)-cholesterol ($r = 0.231$, $P = 0.054$) and non-HDL cholesterol ($r = 0.222$, $P = 0.061$) were close to statistical significance. In line with our previous data, serum FABP4 levels were found to be associated with myocardial neutral lipid content in type 2 diabetes patients ($r = 0.237$, $P = 0.042$) (Fig. 1). Circulating FABP4 was not significantly associated with

Table 1
Spearman's correlations of serum FABP4 with characteristics of study population.

	Non-T2D		T2D	
	r	*P*-value	*r*	*P*-value
Clinical characteristics				
Age	−0.035	0.914	0.071	0.55
Body mass index	−0.483	0.112	−0.01	0.935
Waist circumference	−0.592	0.055	0.359	0.002
Biochemical and metabolomic characteristics				
HbA1c	–	–	0.201	0.086
Plasma fasting glucose	−0.096	0.779	0.095	0.42
Plasma fasting insulin	−0.336	0.312	0.201	0.087
Visceral fat volume	−0.245	0.443	0.383	0.001
Subcutaneous fat volume	−0.462	0.131	0.404	< 0.001
Total cholesterol	0.358	0.28	0.148	0.215
LDL-cholesterol	0.132	0.698	0.231	0.054
HDL-cholesterol	0.538	0.088	−0.235	0.047
Non-HDL-cholesterol	0.145	0.67	0.222	0.61
Plasma NEFA	0.46	0.154	0.059	0.625
Plasma triglycerides	−0.115	0.737	0.16	0.175
Liver triglycerides	−0.063	0.846	0.18	0.127
Leucocyte count	0.5	0.117	0.151	0.206
us-CRP	0.118	0.729	0.09	0.45
Haemodynamic parameters and cardiac dimensions and function				
Systolic blood pressure	–	–	−0.069	0.566
Diastolic blood pressure	–	–	−0.127	0.288
Heart rate	0.102	0.753	−0.214	0.068
LV mass	0.105	0.746	−0.01	0.934
LV end-systolic volume	0.056	0.863	0.066	0.577
LV end-diastolic volume	0.119	0.713	0.033	0.783
Stroke volume	0.322	0.308	−0.007	0.954
LV Ejection fraction	0.231	0.471	0.05	0.671
NT-proBNP	0.055	0.873	0.114	0.334
Cardiac index	0.182	0.572	−0.093	0.429
E peak filling rate	0.084	0.795	0.108	0.358
E-decpeak	−0.172	0.594	−0.069	0.561
E-decmean	−0.136	0.689	−0.087	0.46
E/A peak flow	0.081	0.803	0.085	0.471
Myocardial neutral lipid content	−0.196	0.542	0.237	0.042

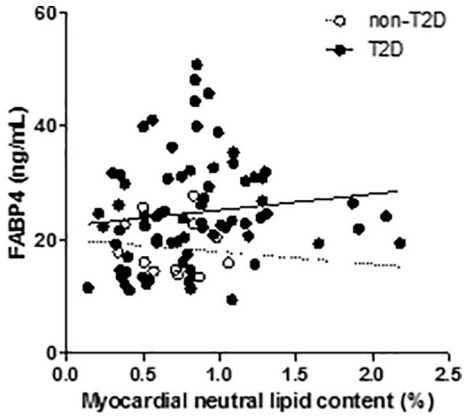

Fig. 1. Circulating FABP4 protein levels are associated with myocardial neutral lipid content in patients with uncomplicated type 2 diabetes. Correlation between the circulating FABP4 levels and the myocardial neutral lipid content (non-T2D: open circles; T2D: closed circles).

any of these parameters in the healthy volunteers. Additional analyses were performed to evaluate the potential role of circulating FABP4 as a biomarker for myocardial neutral lipid content in type 2 diabetes patients.

3.2. Both Circulating FABP4 Protein Levels and Myocardial Neutral Lipids Are Increased in HFD-fed Mice

Next, we used an animal model of insulin resistance induced by HFD. Compared to STD-fed animals, HFD induced insulin resistance, as evidenced by the augmented levels of glucose and insulin, and an increased HOMA-IR index. Coherently, HFD-fed animals became glucose intolerant as indicated by the GTT test. Additionally, HFD-fed mice showed a biochemical profile characteristic of type 2 diabetes, including augmented plasma levels of NEFAs, triglycerides, resistin and leptin, reduced levels of plasma adiponectin (Table S1) and increased myocardial lipid accumulation (Fig. 2A). Based on our data from humans, we analysed FABP4 plasma levels. Additionally, myocardial triglycerides were assessed by LC/MS. Both myocardial triglyceride content and plasma FABP4 levels were increased in the HFD-fed animals compared to animals fed with a STD (Fig. 2B).

3.3. FABP4 Enhances Intramyocellular Lipid Storage and Impairs Fatty Acid Metabolism In HL-1 Cardiomyocytes

Nile red staining revealed that FABP4 induced intracellular lipid content in stimulated cells compared to control cells (~3.1-fold, $P < 0.05$) (Fig. 3A). Using metabolomics approaches, no significant increase in the intracellular triglyceride content was observed between the two conditions (data not shown). Nevertheless, we identified by exact mass 13 lipid species that were upregulated in FABP4-stimulated cells, including phospholipids, vitamin D3 and D6 derivatives, cholesterol derivatives and others (Table S2).

To explore the molecular mechanisms through which FABP4 contributes to intracellular lipid accumulation, we first analysed the expression of genes involved in the fatty acid metabolism. FABP4 did not induce any changes in the mRNA levels of these genes (Fig. 3B). However, the FABP4 protein levels were higher in the plasmatic membrane of FABP4-stimulated cells (~2.3-fold, $P < 0.01$) (Fig. 3C).

3.4. Glucose Metabolism and Insulin Signalling Is Altered in FABP4-Stimulated Cells

Next, we explored whether FABP4 stimulation impacts glucose metabolism. Real-time PCR analysis showed that FABP4 did not alter *Glut4* or *Pdk4* mRNA levels in HL-1 cells (Fig. 4A). However, Western blot

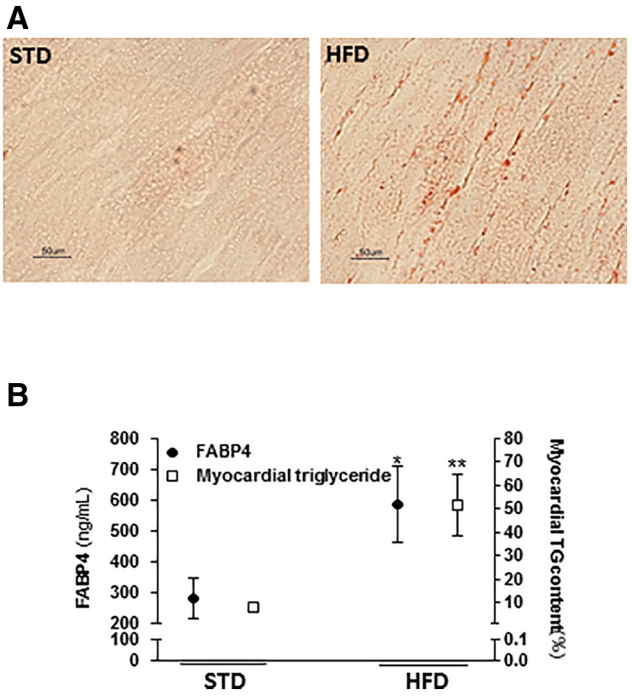

Fig. 2. HFD induced myocardial neutral lipids content and FABP4 plasma levels in C57BL/6J mice. Mice were fed a standard (STD) or high-fat diet (HFD) for 12 weeks. (A) Representative Oil Red O staining in hearts from STD- and HFD-fed animals. (B) Myocardial triglyceride content assessed by LC/MS and FABP4 plasma levels in STD- and HFD-fed animals. Data are expressed as the mean ± SEM. (*$P < 0.05$; **$P < 0.01$ vs. STD-fed animals).

analysis showed that SOCS3 protein levels were induced in FABP4-stimulated cells (Fig. 4B). Accordingly, phosphorylation of STAT3 in Tyr^{705} and Ser^{727} was enhanced after FABP4 challenge (Fig. 4B). Insulin stimulation induced both AKT (~4.4-fold, $P < 0.05$ vs. CT non-stimulated cells) and AS160 (~2.2-fold, $P < 0.05$; vs. CT non-stimulated cells) phosphorylation in non-stimulated cells. Nevertheless, the insulin-induced AKT and AS160 phosphorylation were attenuated in cells challenged with FABP4 (AKT: 31% reduction, $P < 0.05$; vs. CT cells stimulated with insulin. AS160: 29% reduction, $P < 0.05$; vs. CT cells stimulated with insulin) (Fig. 4C and D). Accordingly, the FABP4 challenge prevented insulin-stimulated GLUT4 membrane translocation (Fig. 4E) and glucose uptake (Fig. 4F).

3.5. BMS309403 Reduces FABP4-Induced Lipotoxicity and Improves Insulin Sensitivity in HL-1 Cardiomyocytes

To further analyse the involvement of FABP4 in cardiac fatty acid metabolism, FABP4-challenged cells were treated with the FABP4 inhibitor BMS309403, and the cellular lipid content was analysed. BMS309403 treatment reduced the intracellular lipid content in FABP4-stimulated cells (52% reduction, $P < 0.05$) (Fig. 5A). Among the 13 lipid species identified in FABP4-stimulated cells, 11 were found to be reduced in cells treated with BMS309403 (Table S3). These observations were in line with a slight, but significant reduced the FABP4 membrane protein levels found in cells treated with the FABP4 inhibitor (24% reduction, $P < 0.05$) (Fig. 5B).

Consistent with the observed intracellular lipid reduction, BMS309403 treatment ameliorated the effects of FABP4 on the insulin signalling pathway, enhanced insulin-induced AKT (~1.6-fold, $P < 0.05$; vs. FABP4 cells stimulated with insulin) and AS160 (~1.4-fold, $P < 0.05$; vs. FABP4 cells stimulated with insulin) phosphorylation (Fig. 5C and D, respectively), and glucose uptake (~1.4-fold, $P < 0.05$; vs. FABP4 cells stimulated with insulin) (Fig. 5E).

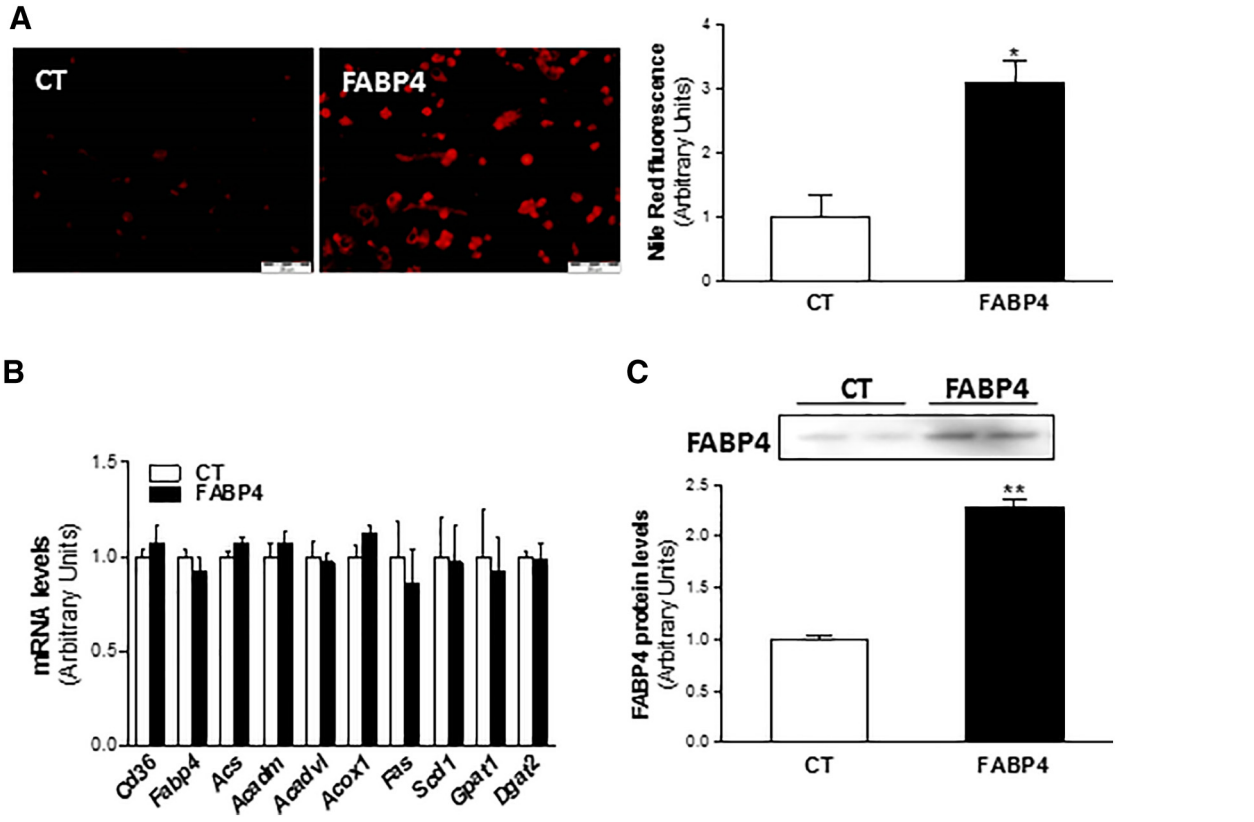

Fig. 3. FABP4 enhances intracellular lipid stores in HL-1 cardiomyocytes. (A) HL-1 cells were stimulated with FABP4 for 24 h, and the intracellular lipid content was analysed by Nile red staining. Representative microphotography showing Nile red fluorescence of lipid droplets (left). Quantification of the Nile red fluorescence intensity (right). (B) HL-1 cells were stimulated with FABP4 for 8 h and the mRNA levels of *Cd36*, *Fabp4*, *Acs*, *Acadm*, *Acadvl*, *Acox1*, *Fas*, *Scd1*, *Gpat1* and *Dgat2* were analysed by real time RT-PCR. Data were normalized to *Tbp* mRNA levels. (C) Western blot showing FABP4 protein levels in the plasma membrane of HL-1 cells stimulated with FABP4 for 24 h. Equal loading was verified by Ponceau staining. Data are expressed as the mean ± SEM (*$P < 0.05$, **$P < 0.01$ vs. CT cells). (For interpretation of the references to colour in this figure legend, the reader is referred to the web version of this article.)

4. Discussion

In this work, we show that circulating FABP4, which is elevated in type 2 diabetic patients, is associated with myocardial neutral lipid content as assessed by ^{1}H-MRS. We validated these data in a murine model of insulin resistance induced by an HFD and explored the potential role of FABP4 as a causal agent for the intracellular lipid accumulation in HL-1 cardiac cells. Using the HL-1 myocardial cell model, we corroborated that exogenous FABP4 increased the amount of intracellular lipids and drove a malfunction in the insulin-signalling pathway that jeopardized glucose uptake. Interestingly, this effect was counterbalanced by the use of the FABP4 inhibitor BMS309403, which lead to decreased intracellular lipid accumulation and improved insulin signalling and glucose uptake in our cellular model.

Since ectopic fat accumulation in heart has been described as one of the main precursors of myocardial dysfunction due to diabetes [9–13], previous studies have focused on the search for new molecules that are useful for identifying patients at increased risk for this disturbance [38]. Nevertheless, so far, none of the molecules that have been proposed as potential biomarkers for myocardial neutral lipid content have been used for the clinical diagnosis of this pathology. Here, we propose FABP4 as an emerging biomarker for myocardial neutral lipid content in type 2 diabetic patients. Similar to increased myocardial neutral lipid content in type 2 diabetic patients, our data revealed that serum FABP4 protein levels were also increased in these patients compared with healthy subjects. These findings were validated in a murine model of insulin resistance induced by an HFD, and increased levels of both plasma FABP4 and myocardial triglycerides were found in HFD-fed mice compared to those animals fed with an STD. In type 2 diabetic patients, but not in the non-diabetic volunteers, FABP4 was found to be statistically associated with cardiac lipid content. Our data are in line with a study performed in non-diabetic subjects that showed no correlation between FABP4 and myocardial triglyceride content in this population, though FABP4 levels were increased in individuals with high myocardial neutral lipid content [57]. These findings support the hypothesis that circulating FABP4 specifically reflects myocardial neutral lipid content in type 2 diabetic subjects, thereby acting as a selective biomarker for these molecules in these individuals. Several studies have found a direct association between circulating FABP4 and heart failure [23,25,29–31]. This association was even higher when only diabetic patients were considered [30]. It is worth noting that in the current study, a population of well-controlled uncomplicated type 2 diabetes patients without clinical evidence of heart failure was studied. In these individuals, FABP4 was not found associated with any parameter that indicates an altered myocardial structure or function, including N-terminal prohormone of brain natriuretic peptide (NT-proBNP), thus indicating that this molecule is able to reflect myocardial neutral lipid content before heart failure is established. Since myocardial lipid accumulation is evident in the absence of heart failure and precedes myocardial dysfunction [11,13], circulating FABP4 may contribute to identification of type 2 diabetic patients with high risk for heart failure, allowing to initiate preventive therapies before alterations in myocardial structure and function occur. The use of FABP4 as an indicator of cardiac lipid levels would be a diagnostic advantage over image-based methods, such as ^{1}H-MRS, since it would be possible to reflect the myocardial neutral lipid content through a well-stablished non-invasive method, both reducing patient discomfort and improving cost-effectiveness. Therefore, circulating FABP4 determination would not only improve the detection of lipid-related cardiac complications but also allow for monitoring of these complications.

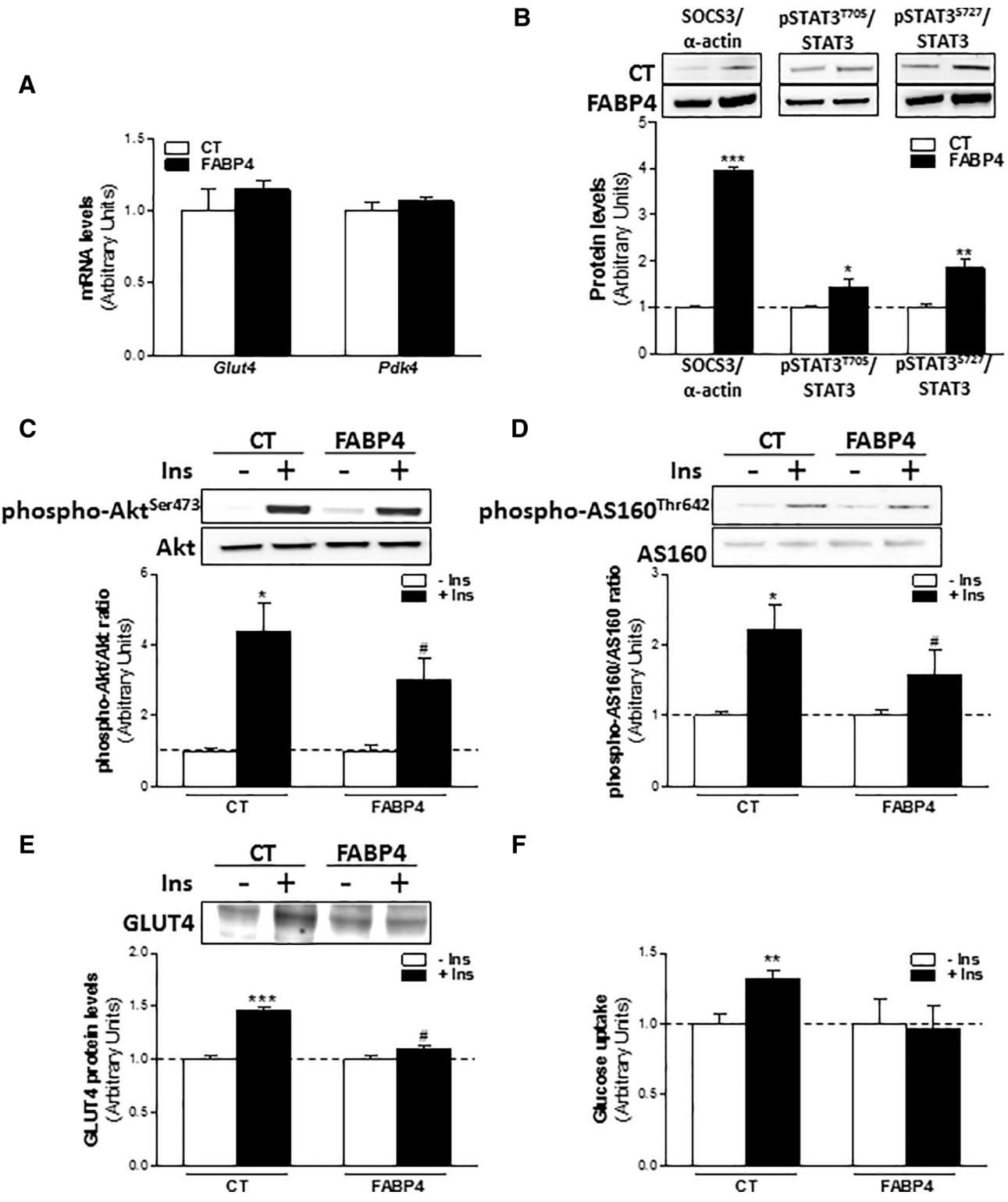

Fig. 4. FABP4 impairs the insulin signalling pathway and glucose uptake in HL-1 cardiomyocytes. (A) Cells were stimulated with FABP4 for 8 h and the mRNA levels of *Glut4* and *Pdk4* were analysed by real time RT-PCR. Data were normalized to *Tbp* mRNA levels. (B) Western blot showing phospho-STAT3^{Tyr705}, phospho-STAT3^{Ser727}, total STAT3 and SOCS3 protein levels in HL-1 cells stimulated with FABP4 for 24 h. To indicate equal loading, the α-actin immunoblot is shown in the same blot. (C—F) HL-1 cells were stimulated with FABP4 for 24 h in the absence (white bars) or presence (black bars) of insulin (200 nmol/l, 10 min). Protein levels of phospho-AKT^{Ser473}, AKT (C), phospho-AS160^{Thr642} and AS160 (D) were analysed by Western blot. Ratios between phosphorylated and total forms of each protein are shown. (E) GLUT4 protein levels in the plasma membrane. Equal loading was verified by Ponceau staining. (F) [^{3}H]-deoxyglucose uptake. Data are expressed as the mean ± SEM. (*$P < 0.05$, ***$P < 0.001$ vs. control cells without insulin stimulation; #$P < 0.05$ control cells stimulated with insulin).

Though our clinical data strongly support serum FABP4 as a molecule reflecting myocardial neutral lipid content in type 2 diabetic patients, this kind of study precludes the establishment of a direct causal relationship between this molecule and myocardial neutral lipid accumulation. Therefore, using HL-1 cardiac cells stimulated with recombinant FABP4, we explored the role of this molecule as a

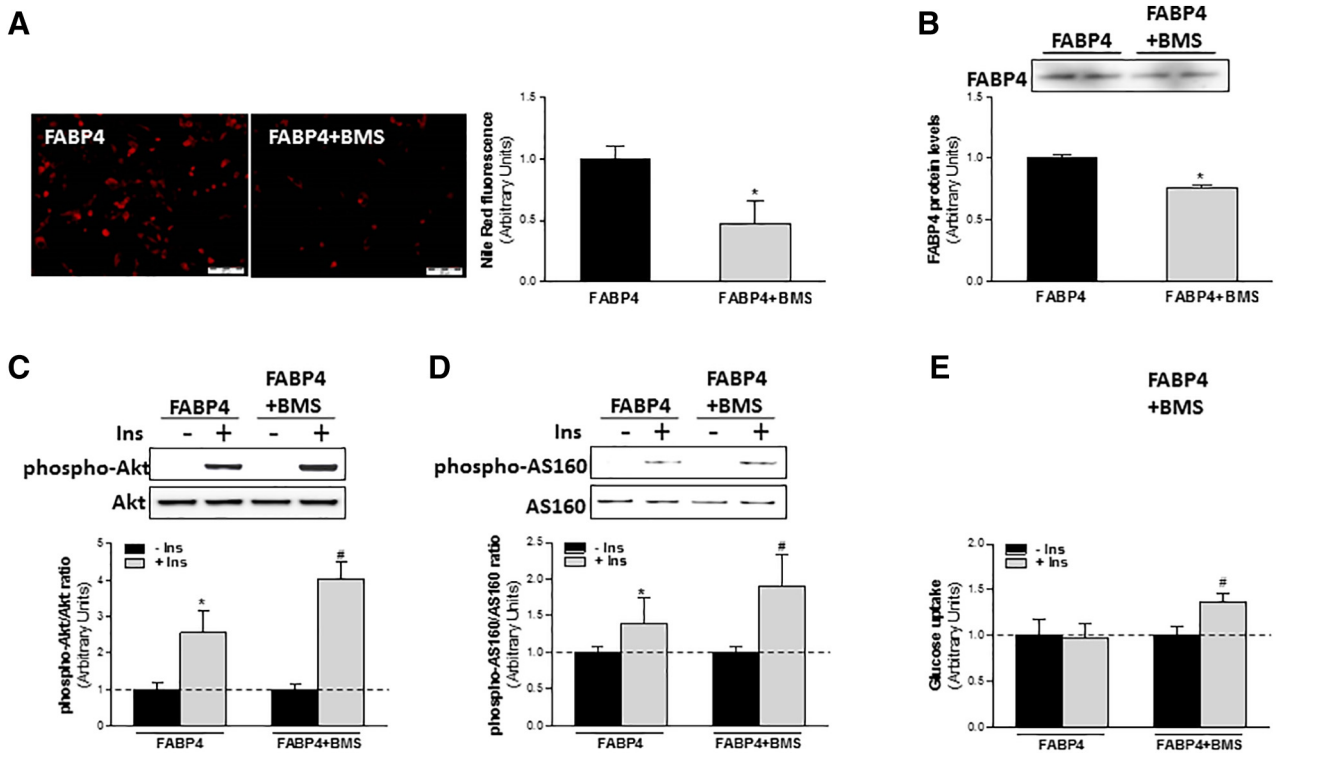

Fig. 5. BMS309403 reduces intracellular lipid stores and restores the insulin signalling pathway and glucose uptake in FABP4-stimulated HL-1 cells. Cells were stimulated with FABP4 for 24 h in the presence or absence of BMS309403, and lipid content was analysed. (A) Representative microphotography showing Nile red fluorescence of lipid droplets (left). Quantification of the Nile red fluorescence intensity (right). (B) Western blot showing the FABP4 protein levels in plasma membrane of HL-1. Equal loading was verified by Ponceau staining. (C–E) FABP4-stimulated cells were treated with BMS309403 in the absence (black bars) or presence (grey bars) of insulin (200 nmol/l, 10 min). Protein levels of phospho-AKT^{Ser473}, AKT (C), phospho-AS160^{Thr642} and AS160 (D) were analysed by Western blot. Ratios between the phosphorylated and total forms of each protein are shown. (E) [^{3}H]-deoxyglucose uptake. Data are expressed as the mean ± SEM of 4 different experiments (*$P < 0.05$ vs. FABP4-stimulated cells or vs. FABP4-challenged cells without insulin stimulation; #$P < 0.05$ FABP4-challenged cells stimulated with insulin).

potential contributor to ectopic fat accumulation in cardiac cells. It has been previously shown that FABP4 increases lipid accumulation in hepatic cells [49]. Here, we found that FABP4 induces intracellular lipid storage in HL-1 cardiomyocytes thus indicating that FABP4 may directly participate in lipid-induced cardiac dysfunction. In particular, our metabolomics approach did not show a significant increase in the intracellular triglyceride content between both groups. This apparently surprising result could be consequence of our experimental conditions, since cells were serum-starved for 24 h before FABP4 stimulation. However, 13 putative lipid species were upregulated in FABP4-stimulated cells, including phospholipids, vitamin D3 and D6 derivatives, cholesterol derivatives and others. FABP4 stimulation did not alter the expression of genes involved in fatty acid uptake, mitochondrial β-oxidation or lipogenesis thus suggesting that this molecule regulates lipid storage through additional mechanisms. Interestingly, Iso et al. showed that FABP4 contributes to trans-endothelial fatty acid transport to cardiomyocytes [36]. Since exogenous FABP4 interacts with plasma membrane proteins in different cell types [58], this may be one of the potential mechanisms by which this protein facilitates fatty acid delivery to cardiomyocytes. Our data reveal that the intracellular lipid stores were related to increased FABP4 plasma membrane protein levels in FABP4-stimulated cells thus suggesting that FABP4 may form complexes involved in fatty acid trafficking across the plasma membrane. Conversely, cells treated with the FABP4 inhibitor BMS309403 showed reduced effects of FABP4 on both lipid stores and FABP4 plasma membrane location. Ectopic fat accumulation in cardiac cells has been related to insulin resistance and altered glucose metabolism [59]. In our cellular model, FABP4 stimulation did not affect *Glut4* and *Pdk4* expression. However, FABP4 induced SOCS3 protein levels and STAT3 phosphorylation, mainly in Ser^{727}. Given that the STAT3/SOCS3 pathway regulates insulin receptor substrate 1 (IRS1) proteasomal degradation [60], FABP4 may directly impact insulin signalling. Accordingly, FABP4 reduced insulin-induced AKT and AS160 phosphorylation, GLUT4 plasma membrane location and glucose uptake. Actually, previous studies from members of our team have shown that FABP4 attenuates insulin signalling in endothelial [61], hepatic [49] and skeletal muscle cells [62]. In line with the observed effects on lipid metabolism, FABP4 inhibition improved insulin sensitivity and glucose uptake in FABP4-challenged HL-1 cardiac cells.

Strengths of our study include the translational approach from experimental models (in vitro and in vivo) to humans (both type 2 diabetic patients and non-diabetic controls). The clinical approach was performed in a well-characterized population, neutral lipid content was determined by ^{1}H-MRS, and there was rigorous control of potential cofounding factors. Clinical data were validated with experimental approaches, which allowed targeting of the molecular mechanisms through which FABP4 contributes to intracellular lipid storage and insulin resistance in cardiac cells. However, some limitations should be taken into account. The clinical studies were performed only in male patients to avoid any possible cofounding effects of hormonal status in females. Subjects included in the study did not show ischaemia or other comorbidities, which allowed evaluation of the effect of diabetes per se on the cardiac lipid content, but precluded extrapolation of the results to other individuals with associated comorbidities. The relatively small sample size attenuated the impact of the results, and the results should be validated in an independent population. In the experimental approaches, the FABP4 inhibitor confirmed the role of FABP4 in cardiac metabolism in the cellular model. However, further research is warranted in animal models before fully considering FABP4 inhibition as a realistic option for the treatment and prevention of lipid-induced cardiac alterations.

5. Conclusions

Altogether, our data identified serum FABP4 as a predictor of myocardial neutral lipid content in type 2 diabetic individuals. In addition, our molecular approach proposed circulating FABP4 not only as a mere biomarker for myocardial lipid accumulation but also as a potential causal agent involved in the development of these processes. The novelty of the current work also lies in the evidence highlighting FABP4 inhibition as an emerging therapeutic strategy against lipotoxicity-induced insulin resistance in cardiac cells. Overall, our findings support FABP4 as a molecular target for early diagnosis and treatment of diabetic cardiomyopathy and lipid-related metabolic disturbances that lead to heart failure.

Author Contribution

RRC conceived the experimental design, conducted, performed and assisted in the experiments, analysed the data and wrote and edited the manuscript. JG contributed to data analysis and review of the manuscript. MR, EB, SGE and MH and took part in the experiments and provided feedback of the manuscript. SS, OY and XC performed metabolomics analysis. RWM, HL, DGC and VLC provided clinical samples, determined analytical parameters and provided feedback of the manuscript. MVC contributed to discussion and review the manuscript. LM applied for funding, directed the study, contributed to discussion, and is the guarantor of this work and, as such, had full access to all the data in the study and takes responsibility for the integrity of the data and accuracy of the data analysis.

Conflict of Interest

The authors declare no conflicts relative to this manuscript.

Funding

This work was supported by funds from Instituto de Salud Carlos III (ISCIII), Madrid, Spain [PI15/00627 to LM and PI14/01729 to VLl—C], Fondo Europeo de Desarrollo Regional [FEDER to LM], the CIBER in Diabetes and Associated Metabolic Disorders [CB07/08/0028 to LM and CB07/08/0003 to MV-C] and CIBER Cardiovascular [CB16/11/00403 to DdG-C and VL-C], the Spanish Ministerio de Economía y Competitividad [SAF2015-64146-R to MV-C and TEC2015-69076-P to XC] and Fundació la Marató de TV3 2014 [to MV-C]. DdG-C was a recipient of Sara Borrell grant from the Instituto de Salud Carlos III Grant [CD14/00109].

Acknowledgments

Authors are grateful for the technical assistance to Yaiza Esteban.

Appendix A. Supplementary Data

Supplementary data to this article can be found online at https://doi.org/10.1016/j.metabol.2019.04.007.

References

[1] Britton KA, Fox CS. Ectopic fat depots and cardiovascular disease. Circulation 2011;124:e837–41.
[2] Lala A, Desai AS. The role of coronary artery disease in heart failure. Heart Fail Clin 2014;10:353–65.
[3] Roberts AW, Clark AL, Witte KK. Review article: left ventricular dysfunction and heart failure in metabolic syndrome and diabetes without overt coronary artery disease—do we need to screen our patients? Diab Vasc Dis Res 2009;6:153–63.
[4] Cohen-Solal A, Beauvais F, Logeart D. Heart failure and diabetes mellitus: epidemiology and management of an alarming association. J Card Fail 2008;14:615–25.
[5] Go AS, Mozaffarian D, Roger VL, Benjamin EJ, Berry JD, Blaha MJ, et al. Executive summary: heart disease and stroke statistics—2014 update: a report from the American Heart Association. Circulation 2014;129:399–410.
[6] Kershaw EE, Flier JS. Adipose tissue as an endocrine organ. J Clin Endocrinol Metab 2004;89:2548–56.
[7] Bonen A, Holloway GP, Tandon NN, Han XX, McFarlan J, Glatz JF, et al. Cardiac and skeletal muscle fatty acid transport and transporters and triacylglycerol and fatty acid oxidation in lean and Zucker diabetic fatty rats. Am J Physiol Regul Integr Comp Physiol 2009;297:R1202–12.
[8] Erion DM, Shulman GI. Diacylglycerol-mediated insulin resistance. Nat Med 2010;16:400–2.
[9] Sharma S, Adrogue JV, Golfman L, Uray I, Lemm J, Youker K, et al. Intramyocardial lipid accumulation in the failing human heart resembles the lipotoxic rat heart. FASEB J 2004;18:1692–700.
[10] Levelt E, Mahmod M, Piechnik SK, Ariga R, Francis JM, Rodgers CT, et al. Relationship between left ventricular structural and metabolic remodeling in type 2 diabetes. Diabetes 2016;65:44–52.
[11] McGavock JM, Lingvay I, Zib I, Tillery T, Salas N, Unger R, et al. Cardiac steatosis in diabetes mellitus: a 1H-magnetic resonance spectroscopy study. Circulation 2007;116:1170–5.
[12] Ng AC, Delgado V, Bertini M, van der Meer RW, Rijzewijk LJ, Hooi Ewe S, et al. Myocardial steatosis and biventricular strain and strain rate imaging in patients with type 2 diabetes mellitus. Circulation 2010;122:2538–44.
[13] Rijzewijk LJ, van der Meer RW, Smit JW, Diamant M, Bax JJ, Hammer S, et al. Myocardial steatosis is an independent predictor of diastolic dysfunction in type 2 diabetes mellitus. J Am Coll Cardiol 2008;52:1793–9.
[14] Rodriguez-Calvo R, Girona J, Alegret JM, Bosquet A, Ibarretxe D, Masana L. Role of the fatty acid-binding protein 4 in heart failure and cardiovascular disease. J Endocrinol 2017;233:R173–84.
[15] Coe NR, Bernlohr DA. Physiological properties and functions of intracellular fatty acid-binding proteins. Biochim Biophys Acta 1998;1391:287–306.
[16] Zimmerman AW, Veerkamp JH. New insights into the structure and function of fatty acid-binding proteins. Cell Mol Life Sci 2002;59:1096–116.
[17] Furuhashi M, Hotamisligil GS. Fatty acid-binding proteins: role in metabolic diseases and potential as drug targets. Nat Rev Drug Discov 2008;7:489–503.
[18] Furuhashi M, Ishimura S, Ota H, Miura T. Lipid chaperones and metabolic inflammation. Int J Inflamm 2011;2011:642612.
[19] Kralisch S, Fasshauer M. Adipocyte fatty acid binding protein: a novel adipokine involved in the pathogenesis of metabolic and vascular disease? Diabetologia 2013;56:10–21.
[20] Tso AW, Xu A, Sham PC, Wat NM, Wang Y, Fong CH, et al. Serum adipocyte fatty acid binding protein as a new biomarker predicting the development of type 2 diabetes: a 10-year prospective study in a Chinese cohort. Diabetes Care 2007;30:2667–72.
[21] Xu A, Tso AW, Cheung BM, Wang Y, Wat NM, Fong CH, et al. Circulating adipocyte-fatty acid binding protein levels predict the development of the metabolic syndrome: a 5-year prospective study. Circulation 2007;115:1537–43.
[22] Cabre A, Lazaro I, Girona J, Manzanares JM, Marimon F, Plana N, et al. Fatty acid binding protein 4 is increased in metabolic syndrome and with thiazolidinedione treatment in diabetic patients. Atherosclerosis 2007;195:e150–8.
[23] Fuseya T, Furuhashi M, Yuda S, Muranaka A, Kawamukai M, Mita T, et al. Elevation of circulating fatty acid-binding protein 4 is independently associated with left ventricular diastolic dysfunction in a general population. Cardiovasc Diabetol 2014;13:126.
[24] Baessler A, Lamounier-Zepter V, Fenk S, Strack C, Lahmann C, Loew T, et al. Adipocyte fatty acid-binding protein levels are associated with left ventricular diastolic dysfunction in morbidly obese subjects. Nutr Diabetes 2014;4:e106.
[25] Balci MM, Arslan U, Firat H, Kocaoglu I, Vural MG, Balci KG, et al. Serum levels of adipocyte fatty acid-binding protein are independently associated with left ventricular mass and myocardial performance index in obstructive sleep apnea syndrome. J Invest Med 2012;60:1020–6.
[26] Engeli S, Utz W, Haufe S, Lamounier-Zepter V, Pofahl M, Traber J, et al. Fatty acid binding protein 4 predicts left ventricular mass and longitudinal function in overweight and obese women. Heart 2013;99:944–8.
[27] Huang CL, Wu YW, Wu CC, Lin L, Wu YC, Hsu PY, et al. Association between serum adipocyte fatty-acid binding protein concentrations, left ventricular function and myocardial perfusion abnormalities in patients with coronary artery disease. Cardiovasc Diabetol 2013;12:105.
[28] Liu M, Zhou M, Bao Y, Xu Z, Li H, Zhang H, et al. Circulating adipocyte fatty acid-binding protein levels are independently associated with heart failure. Clin Sci 2013;124:115–22.
[29] Tang WH, Francis GS, Morrow DA, Newby LK, Cannon CP, Jesse RL, et al. National Academy of Clinical Biochemistry Laboratory Medicine practice guidelines: clinical utilization of cardiac biomarker testing in heart failure. Circulation 2007;116:e99–109.
[30] Cabre A, Valdovinos P, Lazaro I, Bonet G, Bardaji A, Masana L. Parallel evolution of circulating FABP4 and NT-proBNP in heart failure patients. Cardiovasc Diabetol 2013;12:72.
[31] Djousse L, Bartz TM, Ix JH, Kochar J, Kizer JR, Gottdiener JS, et al. Fatty acid-binding protein 4 and incident heart failure: the Cardiovascular Health Study. Eur J Heart Fail 2013;15:394–9.
[32] Vural B, Atalar F, Ciftci C, Demirkan A, Susleyici-Duman B, Gunay D, et al. Presence of fatty-acid-binding protein 4 expression in human epicardial adipose tissue in metabolic syndrome. Cardiovasc Pathol 2008;17:392–8.
[33] Zhang J, Qiao C, Chang L, Guo Y, Fan Y, Villacorta L, et al. Cardiomyocyte overexpression of FABP4 aggravates pressure overload-induced heart hypertrophy. PLoS One 2016;11:e0157372.
[34] Zhou M, Bao Y, Li H, Pan Y, Shu L, Xia Z, et al. Deficiency of adipocyte fatty-acid-binding protein alleviates myocardial ischaemia/reperfusion injury and diabetes-induced cardiac dysfunction. Clin Sci 2015;129:547–59.
[35] Lamounier-Zepter V, Look C, Alvarez J, Christ T, Ravens U, Schunck WH, et al. Adipocyte fatty acid-binding protein suppresses cardiomyocyte contraction: a new link between obesity and heart disease. Circ Res 2009;105:326–34.

[36] Iso T, Maeda K, Hanaoka H, Suga T, Goto K, Syamsunarno MR, et al. Capillary endothelial fatty acid binding proteins 4 and 5 play a critical role in fatty acid uptake in heart and skeletal muscle. Arterioscler Thromb Vasc Biol 2013;33:2549–57.
[37] van der Meer RW, Rijzewijk LJ, de Jong HW, Lamb HJ, Lubberink M, Romijn JA, et al. Pioglitazone improves cardiac function and alters myocardial substrate metabolism without affecting cardiac triglyceride accumulation and high-energy phosphate metabolism in patients with well-controlled type 2 diabetes mellitus. Circulation 2009; 119:2069–77.
[38] de Gonzalo-Calvo D, van der Meer RW, Rijzewijk LJ, Smit JW, Revuelta-Lopez E, Nasarre L, et al. Serum microRNA-1 and microRNA-133a levels reflect myocardial steatosis in uncomplicated type 2 diabetes. Sci Rep 2017;7:47.
[39] Paelinck BP, de Roos A, Bax JJ, Bosmans JM, van Der Geest RJ, Dhondt D, et al. Feasibility of tissue magnetic resonance imaging: a pilot study in comparison with tissue Doppler imaging and invasive measurement. J Am Coll Cardiol 2005;45:1109–16.
[40] van der Meer RW, Hammer S, Smit JW, Frolich M, Bax JJ, Diamant M, et al. Short-term caloric restriction induces accumulation of myocardial triglycerides and decreases left ventricular diastolic function in healthy subjects. Diabetes 2007;56:2849–53.
[41] Vanhamme L, van den Boogaart A, Van Huffel S. Improved method for accurate and efficient quantification of MRS data with use of prior knowledge. J Magn Reson 1997;129:35–43.
[42] van der Meer RW, Doornbos J, Kozerke S, Schar M, Bax JJ, Hammer S, et al. Metabolic imaging of myocardial triglyceride content: reproducibility of 1H MR spectroscopy with respiratory navigator gating in volunteers. Radiology 2007;245:251–7.
[43] van der Meer RW, Diamant M, Westenberg JJ, Doornbos J, Bax JJ, de Roos A, et al. Magnetic resonance assessment of aortic pulse wave velocity, aortic distensibility, and cardiac function in uncomplicated type 2 diabetes mellitus. J Cardiovasc Magn Reson 2007;9:645–51.
[44] Furuhashi M, Tuncman G, Gorgun CZ, Makowski L, Atsumi G, Vaillancourt E, et al. Treatment of diabetes and atherosclerosis by inhibiting fatty-acid-binding protein aP2. Nature 2007;447:959–65.
[45] Matthews DR, Hosker JP, Rudenski AS, Naylor BA, Treacher DF, Turner RC. Homeostasis model assessment: insulin resistance and beta-cell function from fasting plasma glucose and insulin concentrations in man. Diabetologia 1985;28:412–9.
[46] Rodriguez-Calvo R, Vazquez-Carrera M, Masana L, Neumann D. AICAR protects against high palmitate/high insulin-induced intramyocellular lipid accumulation and insulin resistance in HL-1 cardiac cells by inducing PPAR-target gene expression. PPAR Res 2015;2015:785783.
[47] Rodriguez-Calvo R, Chanda D, Oligschlaeger Y, Miglianico M, Coumans WA, Barroso E, et al. Small heterodimer partner (SHP) contributes to insulin resistance in cardiomyocytes. Biochim Biophys Acta 2017;1862:541–51.
[48] Mehlem A, Hagberg CE, Muhl L, Eriksson U, Falkevall A. Imaging of neutral lipids by oil red O for analyzing the metabolic status in health and disease. Nat Protoc 2013;8:1149–54.
[49] Bosquet A, Guaita-Esteruelas S, Saavedra P, Rodriguez-Calvo R, Heras M, Girona J, et al. Exogenous FABP4 induces endoplasmic reticulum stress in HepG2 liver cells. Atherosclerosis 2016;249:191–9.
[50] Smith CA, Want EJ, O'Maille G, Abagyan R, Siuzdak G. XCMS: processing mass spectrometry data for metabolite profiling using nonlinear peak alignment, matching, and identification. Anal Chem 2006;78:779–87.
[51] Vinaixa M, Samino S, Saez I, Duran J, Guinovart JJ, Yanes O. A guideline to univariate statistical analysis for LC/MS-based untargeted metabolomics-derived data. Metabolites 2012;2:775–95.
[52] Rodriguez-Calvo R, Guadall A, Calvayrac O, Navarro MA, Alonso J, Ferran B, et al. Over-expression of neuron-derived orphan receptor-1 (NOR-1) exacerbates neointimal hyperplasia after vascular injury. Hum Mol Genet 2013;22:1949–59.
[53] Calvayrac O, Rodriguez-Calvo R, Marti-Pamies I, Alonso J, Ferran B, Aguilo S, et al. NOR-1 modulates the inflammatory response of vascular smooth muscle cells by preventing NFkappaB activation. J Mol Cell Cardiol 2015;80:34–44.
[54] Glass R, Loesch A, Bodin P, Burnstock G. P2X4 and P2X6 receptors associate with VE-cadherin in human endothelial cells. Cell Mol Life Sci 2002;59:870–81.
[55] Jove M, Planavila A, Laguna JC, Vazquez-Carrera M. Palmitate-induced interleukin 6 production is mediated by protein kinase C and nuclear-factor kappaB activation and leads to glucose transporter 4 down-regulation in skeletal muscle cells. Endocrinology 2005;146:3087–95.
[56] Jonker JT, Lamb HJ, van der Meer RW, Rijzewijk LJ, Menting LJ, Diamant M, et al. Pioglitazone compared with metformin increases pericardial fat volume in patients with type 2 diabetes mellitus. J Clin Endocrinol Metab 2010;95:456–60.
[57] Graner M, Gustavsson S, Nyman K, Siren R, Pentikainen MO, Lundbom J, et al. Biomarkers and prediction of myocardial triglyceride content in non-diabetic men. Nutr Metab Cardiovasc Dis 2016;26:134–40.
[58] Saavedra P, Girona J, Bosquet A, Guaita S, Canela N, Aragones G, et al. New insights into circulating FABP4: interaction with cytokeratin 1 on endothelial cell membranes. Biochim Biophys Acta 2015;1853:2966–74.
[59] Borradaile NM, Schaffer JE. Lipotoxicity in the heart. Curr Hypertens Rep 2005;7: 412–7.
[60] Rui L, Yuan M, Frantz D, Shoelson S, White MF. SOCS-1 and SOCS-3 block insulin signaling by ubiquitin-mediated degradation of IRS1 and IRS2. J Biol Chem 2002;277: 42394–8.
[61] Aragones G, Saavedra P, Heras M, Cabre A, Girona J, Masana L. Fatty acid-binding protein 4 impairs the insulin-dependent nitric oxide pathway in vascular endothelial cells. Cardiovasc Diabetol 2012;11:72.
[62] Bosquet A, Girona J, Guaita-Esteruelas S, Heras M, Saavedra-Garcia P, Martinez-Micaelo N, et al. FABP4 inhibitor BMS309403 decreases saturated-fatty-acid-induced endoplasmic reticulum stress-associated inflammation in skeletal muscle by reducing p38 MAPK activation. Biochim Biophys Acta 2018;1863:604–13.